

Diagnosis of the behavior characteristics of the evaporative diesel spray by using images analysis

Jeongkuk Yeom*

Division of Mechanical Engineering, Dong-A University, Busan 604-714, Korea

(Manuscript Received August 10, 2007; Revised May 5, 2008; Accepted June 4, 2008)

Abstract

In this study, the effects of change in injection pressure on spray structure have been investigated on the high temperature and pressure field. To analyze the structure of evaporative diesel spray is important in speculation of mixture formation process. Also emissions of diesel engines can be controlled by the analyzed results. Therefore, this study examines the evaporating spray structure in a constant volume chamber. The injection pressure is selected as the experimental parameter, is changed from 72 MPa to 112 MPa with a high pressure injection system (ECD-U2). The PIV (Particle Image Velocimetry) technique was used to capture behavior variation of the evaporative diesel spray. Analysis of the mixture formation process of diesel spray was executed by the results of flow analysis in this study. Consequentially the large-scale vortex flow could be found in downstream spray and the formed vortex governs the mixture formation process in diesel spray.

Keywords: Spray structure; Mixture formation; Evaporative diesel spray; Vortex; PIV technique

1. Introduction

The major technology for enhancing the efficiency of automobile engines today is the direct injection of gasoline engine and diesel engine. The direct injection technique of fuel into in-cylinder has brought about the realization of various mixture formation mechanisms. An example of a direct gasoline injection engine is the realization of stratified combustion from variable mixture degree of fuel and air which can be achieved through the injecting fuel among the existing intake air into the cylinder during compression stroke [1]. So far, direct injection was the mainstream system used in diesel engines, however, nowadays the trend of injection technique is shifting towards using high pressure due to its many merits, including enhancement of combustion efficiency and reduction of particulate matters from emission gas. However, there is a problem in that the amount of

nitrogen oxide (NO_x) produced as a result of the high temperature of combustion gas increases. Thus, it is necessary to find a way to reduce production of NO_x by controlling the mixture either by reducing the injection duration or through pilot injection. In this regard, even with respect to the diesel engines, great attention is being drawn to developing a method for controlling the combustion level through optimization of the mixture, it is important to study the mixture formation structure which is based on the diesel spray structure. In this paper, we shall attempt to explain the evaporating diesel free spray structure at high temperature · high pressure field to control the mixture formation more efficiently. An analysis on the evaporating diesel spray structure was conducted through the flow analysis of the spray, which was conducted using a particle image velocimetry (PIV) [2] and setting the measured region as the downstream region of the evaporating spray where the mixture of the fuel and ambient gas is most vigorous. In terms of the experimental condition, the injection pressure was varied.

*Corresponding author. Tel.: +82 51 200 7640, Fax.: +82 51 200 7656
E-mail address: laser355@dau.ac.kr
© KSME & Springer 2008

2. Experiment apparatus and procedure

2.1 Optical system of mie scattering light

Fig. 1 shows a PIV optical system using droplet Mie scattering light signal emitted from laser sheet light. An Nd:YAG Spectra-Physics system (PIV400) as the visual measurement apparatus was used in this study. Two Nd:YAG lasers (GCR170) were installed as a light source in the laser system PIV400. The emitted two laser lights were reflected on the high-frequency generator (Quanta-Ray:HG-2) and re-emitted as second harmonic laser light with a wavelength of 532 nm. The $\Phi 10$ mm circular beam was passed through a pin hole and transformed into a $\Phi 5$ mm circular beam. Then, the beam was passed through an $f15$ mm cylindrical lens and transformed into an elliptical thin sheet, and then, passed through an $f1000$ mm and condensed into a sheet light. The width and thickness of obtained laser sheet beam were 100 mm and approximately 0.2 mm when the laser light passes the constant volume chamber. In the capturing process, a high resolution and high frame-rate digital image processing system was used, which is composed of a computer equipped with a cross correlation camera (TSI:PIVCAM10-30), a laser pulse synchronizer (TSI:model-610032) and a PIV analysis software (TSI:INSIGHT3). The laser pulse synchronizer is controlled by INSIGHT3. By using the laser pulse synchronizer, two consecutive images can be obtained within the set time by the controlling the emitting laser light and the shutter timing of the camera. A laser cross correlation camera was installed such that it is perpendicular to the laser sheet light, and the light signals that penetrate through the object lens were captured on the CCD camera. The pixel array size and the spatial resolution of the cross correlation camera was 1000×1012 pixels and 0.06

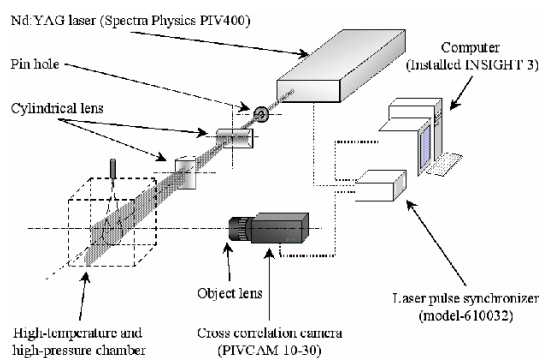


Fig. 1. Schematic diagram of laser sheet optical system.

mm/pixel, respectively. The fuel used in the experiment was n-Tridecane ($C_{13}H_{28}$, degree of purity 99 %) and the ambient gas (Nitrogen gas : N_2), was charged into the experiment chamber.

2.2 Fuel injection system

Fig. 2 shows fuel injection system of an electric control accumulator type, ECD-U2, manufactured by Denso Co., Ltd. ECD-U2 [3] is consisted of a high pressure pump, common rail, injector, and an ECU and a sensor to control the aforementioned instruments. The fuel pressure within the common rail regulates the high pressure pump fuel discharge amount by increasing and decreasing the frequency of the opening and closing of the pump control valve (PCV). The fuel within the common rail of which the pressure is maintained as set up pressure is introduced into the injector via a flow damper. A 3-dimensional electric valve is installed in the injector that controls the injection rate by the needle valve orifice. The used diffusion nozzle was a single hole nozzle with a diameter of 0.2 mm and length of 1.0 mm ($[l/d]=5.0$).

2.3 Experiment conditions

Table 1 presents the experimental conditions. The ambient condition inside the chamber is the same high temperature · pressure ambient condition of the cylinder at the initial injection of high speed diesel engine with direct injection system. The ambient temperature (T_a) was set as 700 K, the ambient pressure as 2.55 MPa, the ambient density (ρ_a) as 12.3 kg/m^3 . The injection duration for the injection pressure (p_{inj}), 72 MPa and 112 MPa were 1.54 ms and 1.24 ms, respectively. The injection quantity for each pressure

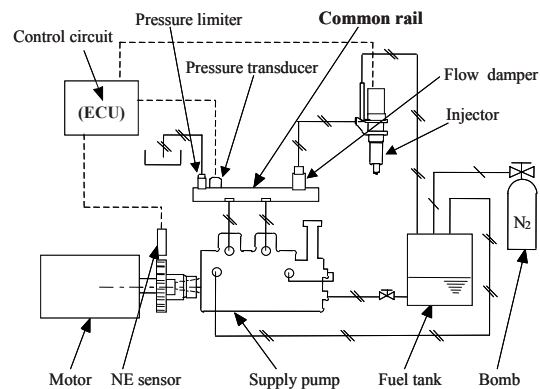


Fig. 2. Schematic diagram of ECD-U2 system.

Table 1. Experimental conditions.

Injection nozzle	Diameter of hole d_n [mm]	0.2
	Length of hole L_n [mm]	1.0
Ambient gas		N ₂ gas
Ambient temperature	T_a [K]	700
Ambient pressure	P_a [MPa]	2.55
Ambient density	ρ_a [kg/m ³]	12.3
Injection pressure	P_{inj} [MPa]	72, 112
Injection quantity	Q_{inj} [mg]	12.0
Injection duration	t_{inj} [ms]	1.54, 1.24

was 12 mg for both cases. In addition, the injection system that was used in this experiment showed a square shaped injection rate, and the injection quantity for each capture time (i.e., 2/4, 3/4 and 4/4 t/t_{inj} , dimensionless time) were found to be the same. Prior to conducting the actual experiment, the reproducibility of the injected fuel spray could be fully confirmed.

2.4 Principle of particle image velocimetry (PIV)

PIV measurement is a technique of measuring the phenomenon transfer at the region where the cross correlation coefficient, which is obtained from the brightness of the 2-images captured within a set short time period, is the highest. It is through this method that the degree of movement and change of such movement within the spray can be determined. In this study, we obtained numerical data, such as 0 bit, to denote the dark area and 8 bits (256 gradients) to denote the bright area within the spray.

Fig. 3 shows a flow chart for the PIV analysis, and the next equation was used to obtain the vorticity distribution, which is important in understanding more about the vortex flow within the spray.

$$\omega = \frac{\partial u_z}{\partial R} - \frac{\partial u_R}{\partial Z}$$

where, u_z is velocity of the spray axial direction, u_R is velocity of the spray radial direction, Z is distance from nozzle tip and R is radial distance from spray axis.

2.5 Flow observation of tracer for PIV measurement

In order to observe flow of the ambient gas, a tracer was used to mix the seed particles (Lumilight Pigment : Red, mean diameter 2~8 μm , specific gravity 4, thermostable temperature: 1023 K) with ambient gas by using the agitational fan prior to the injection of

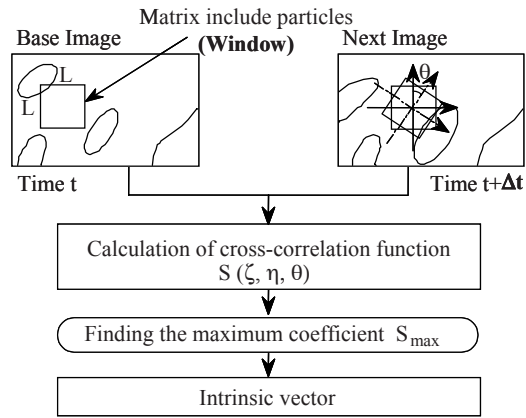


Fig. 3. Flow chart of cross-correlation.

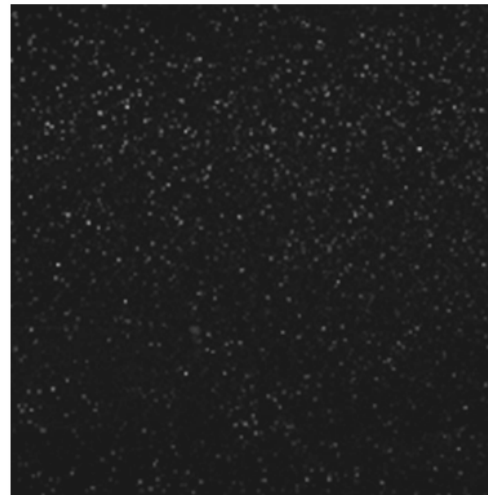


Fig. 4. Seed particle image before PIV measurement.

fuel. Fig. 4 shows the distribution of the seed particle within the chamber. From this image, it can be seen that the seed particles from the images are uniformly distributed throughout the investigated region. Furthermore, when this image was used in PIV measurement any flow of the seed particles could not be observed during the period ($\Delta t = 7 \mu\text{s}$) of the two captured images. Consequently, the flow of seed particle could be ignored when studying the flow of the spray ambient gas in this study.

3. Results and discussion

3.1 Analysis of the flow of spray ambient gas

Figs. 5 and 6 show the velocity distribution of the ambient gas obtained from the 2-dimensional section

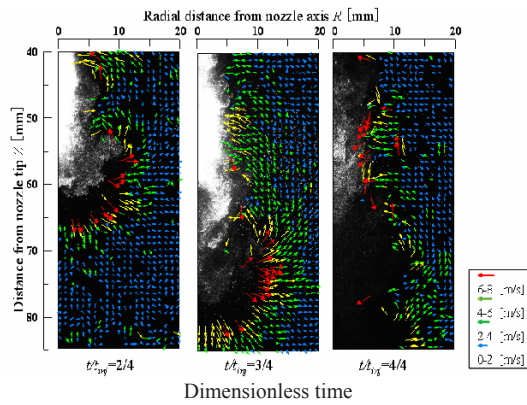


Fig. 5. Temporal change in velocity distribution of ambient gas taken by PIV ($p_{inj}=72$ [MPa], $t_{inj}=1.54$ [ms]).

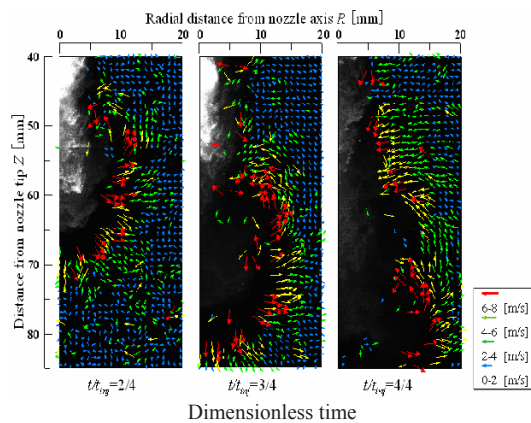


Fig. 6. Temporal change in velocity distribution of ambient gas taken by PIV ($p_{inj}=112$ [MPa], $t_{inj}=1.24$ [ms]).

images of the spray liquid-phase. The y-axis represents the distance from injection nozzle tip, Z , the x-axis represents the radial distance from the spray central axis in the figures. Although the scattering signal of the particles is used as tracer, not only must the ambient gas seed particle be measured but also the droplet scattering light signal within the injected spray in this study. However, the velocity (V m/s) of the droplets within the spray liquid-phase is much faster compared with that of the spray ambient gas. Thus, the velocity of $V \geq 8.0$ m/s was excluded by the range cut from difference in velocity between the spray liquid-phase and the ambient gas. In Fig. 6, where the injection pressure is high as $p_{inj}=112$ MPa, the gap can be found between the spray liquid-phase image and velocity vectors of ambient particle. It can be speculated that there is droplets with low scattering

brightness in evaporating spray region. It can be easily seen that the gap in Fig. 6 is wider than that in Fig. 5. Moreover, considering that the entire liquid-phase scattering brightness is low and the fact that the gap is obvious at the edge of the spray liquid-phase, the atomization of the droplets is promoted by the high pressure injection. It can be concluded that the shear action between ambient gas and injected spray in the surrounding area of the spray liquid-phase and the ensuing vortex motion are the causes of the spray evaporation · diffusion to occurring vigorously. In addition, the branch-like structure that is illuminated in the non-evaporated spray [4], which is the rugged area at the spray edge, is formed by the initial perturbation that occur as a result of the interaction between the spray and the ambient gas in the upper spray region. This kind of branch-like structure may bring about heterogeneous mixture inside the spray, and consequently, as it flows to the lower spray region, it develops into greater vortex motion that determines the formation characteristics of the mixture of the diesel spray. In the case of the seed flow, with respect to each injection condition $t/t_{inj} = 2/4$ and $t/t_{inj} = 3/4$ based on the liquid-phase tip, it can be observed that the ambient gas flows into the spray at the upper region and flows into the direction of spray growth the spray at the lower region. Therefore, the ambient gas is entrained into the upper spray region and at the same time, this flow with high flow velocity becomes dominated by the vortex motion that develops in the surrounding area of the spray. Then, there is a large vector in the velocity of the spray development direction at the spray tip, and, in the same spray tip region, the spray flow have a value of velocity component in the radial direction as a result of the resistance by the ambient gas.

3.2 Statistical analysis of ambient gas flow

Fig. 7 shows the mean velocity of the spray axial direction, V_z , which is the average value for ambient gas velocities, u_z , obtained from experiment of 5 times under the same conditions with respect to the position of Z in each axial direction.

Fig. 8 shows the mean velocity of the spray radial direction, V_r , of the ambient gas obtained with the same method used for Fig. 7. In the x-axis, also we used the value from the measured location divided by the length of spray penetration, L_{liq} , in order to clearly show the relation between the change in velocity and

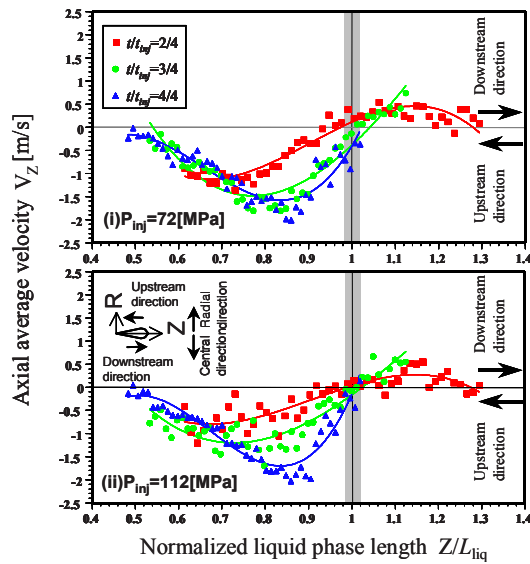


Fig. 7. Change in average velocity at axial direction.

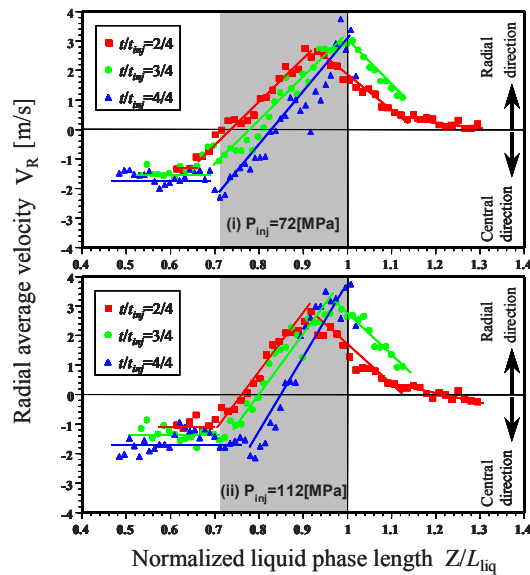


Fig. 8. Change in average velocity at radial direction.

the liquid-phase tip. However, if the experiment is conducted in the evaporating field as in this study, it would be difficult to measure the liquid-phase length of the spray because the scattering brightness of the droplets dramatically changes. Therefore, the penetration length of liquid spray used based on the result of the experiment by Yeom et al. [5] where the exciplex fluorescence method was used as follows: $L_{liq} = 65$ mm at $t/t_{inj} = 2/4$, $L_{liq} = 75$ mm at $t/t_{inj} = 3/4$ and $L_{liq} = 83$ mm at $t/t_{inj} = 4/4$. The y-axis represents the mean

velocity. In Fig. 7, the spray axial direction is denoted as positive whereas in Fig. 8, the radial direction from the central axis of the spray is also denoted as positive. Although a large ambient gas flow moving from the spray tip to the upper stream can be seen in Figs. 5 and 6, the turning point of the liquid-phase can be found at the upper liquid-phase region ($Z/L_{liq} = 1$) as shown in Fig. 7. From Figs. 7 and 8, the overall trend and the region of the mean velocity with respect to each injection condition is the similar, however, the variation of each velocity component value is remarkable in the case of high pressure injection. Here, since the change in the ambient gas velocity is correlated with the degree of the change of the ambient gas flow, the sample displacement coefficient [6] of the mean velocity illustrating the change in the values is used in Figs. 7 and 8.

Also the change in the mean velocity due to the difference in the injection pressure quantitatively is shown in Fig. 9. In the figure, (a) and (b) represents the sample coefficients of the axial direction velocity component, V_R , and the radial direction velocity component, V_Z , respectively. The change in axial direction velocity in (a) is few in the high pressure injection region at capture time, $t/t_{inj} = 2/4$ and $3/4$. However, in the case of each capture time in (b), the radial direction velocity changes dramatically in the high pressure injection at each capture time. Such result of the radial direction velocity shows a contrasting tendency with that of (a). Diffusion phenomenon can be categorized as molecular diffusion due to the heat motion of the molecules and turbulence diffusion ([or vortex diffusion]) [7] that form due to the vortex from fluid flow. In spray diffusion phenomenon, the turbulence diffusion is more dominant. Turbulence diffusion means the movement of the flow characteristics in the vertical directions following the vortex movement. We believe that the direction perpendicular to the flow, that is, the velocity of the spray radial direction shall be said to have a correlation with the turbulence diffusion phenomenon and as a result of which, the increase in the injection pressure shall represent the increase in the vortex of the ambient gas. Therefore, even though each behavior characteristics of the mean velocity change in Figs. 7 and 8 show the same tendency from a macro perspective, irrespective of the injection pressure, the increase in the injection pressure from the change in the value as shown in Fig. 9 is assumed to influence the vortex motion that dominates the ambient gas flow. From the above

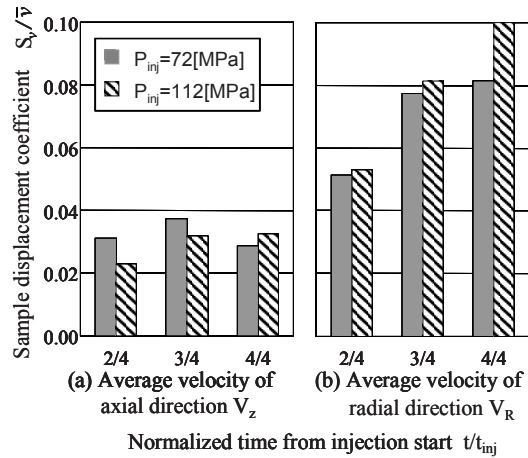


Fig. 9. Change in sample displacement coefficient.

results, if the fuel mass within the spray is the same, the change in the macro-flow characteristics of the spray show the same behavior irrespective of the injection pressure. Also the increase in injection pressure causes a more turbulent flow in ambient gas, making it possible to rapidly form mixture of diesel spray. On the one hand, the radial direction velocity passing $v = 0$ linearly increase at each time $Z/L_{liq} = 0.7\sim 1$. Such velocity gradient is a clear indication of the vortex motion in the ambient gas. Also, it can be found that the size of the vortex is approximately 30% that of the length of spray penetration because a steep velocity gradient exist at time $Z/L_{liq} = 0.7\sim 1$. With respect to the non-evaporative spray structure, Takagishi et al. [8] reported that the size of the vortex structure formed in the vicinity of nozzle grows in accordance with the flow of the spray to the downstream region, and at the spray tip region, the size of the vortex structure reaches the spray radius, in other words, two vortex arrays is made by interaction between injected spray and ambient gas in the vertical section of spray. Based on this point, it can be speculated that there exist a large size vortex structure, which is approximately as large as 30% of the length of spray penetration at the tip region of the evaporative diesel free spray. Also if the fuel mass within the spray is the same, the injection pressure has no effect on the size of the vortex structure.

Fig. 10 shows the results obtained from the PIV analysis where the Mie scattering signal of liquid-phase spray was used as a tracer. Among the figures, (a) shows the scattering signal of liquid-phase spray, (b) shows the distribution of velocity vector and (c)

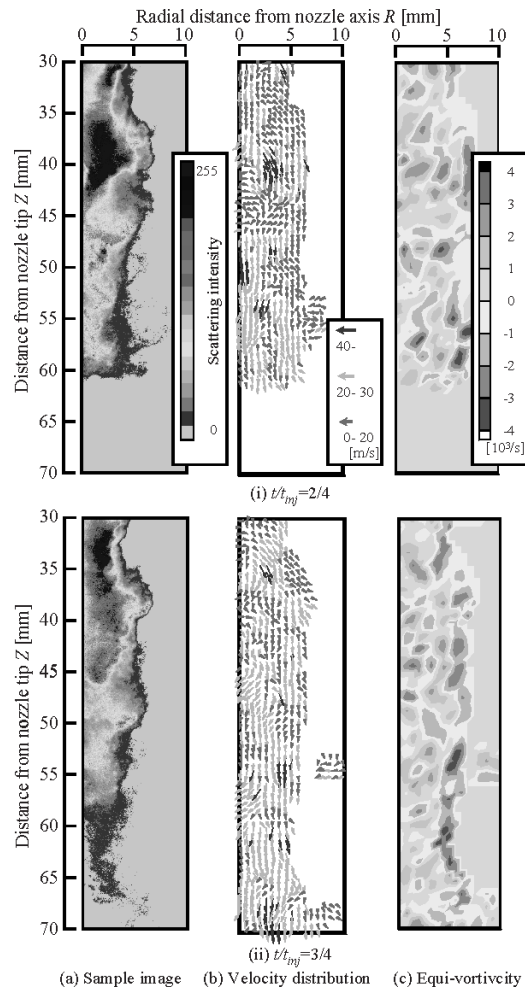


Fig. 10. Calculated results for velocity and vorticity by PIV($p_{inj}=72$ [MPa], $t_{inj}=1.54$ [ms]).

shows the vorticity distribution. The time interval between the two images was set to $\Delta t=5 \mu s$. Image (a) was changed from the 256 gradations (8 bit) to a 20 gradations color image so that the droplets diameter or density distribution is more obvious. Tanaka [9] conducted analysis on the evaporative spray flow under the same conditions as this study, and they defined the turning point of the liquid-phase spray flow as $Z = 56$ mm in direction of axis. In other words, up to $Z = 56$ mm from the nozzle outlet, the main flow of the liquid-phase spray can be found around the vortex structure. The main flow is meandered by two vortex arrays on both sides. Consequently, the spray flow becomes complex owing to the mixing the motion of separated vortex at the downstream region of the spray. Takahashi [10] set

the distance up to the nozzle outlet of $Z = 38$ mm as the liquid-phase length and defined such region where the momentum exchange vigorously occurs between injected spray and ambient gas. From Fig. 10-(a), the continuous bright region occurs in the spray central axis up to $Z = 50$ mm of the liquid-phase image, and in the downstream region, that is, the region near the edges of the spray and lower than $Z = 50$ mm, the change in the brightness is more obvious. In Fig. 10-(b), through the analysis on the correlation of velocity vector, it can be found that there are many velocity vectors in the region with high scattering brightness. Also, the fluctuation of the velocity vector is keener in the region where the change in brightness of image is obvious and vortex flow can be seen in local region. From Fig. 10-(c) of the vorticity distribution, there is strong vorticity of $\omega < -3000$ 1/s like a wall in the spray edge. Then it can be speculated that the diffusion is vigorous at the spray edge due to the interaction between the spray and the ambient gas. The high vorticity region can be seen at local part of the spray downstream region. Also, the flow of fuel droplets obeys to flow of ambient gas due to the momentum reduction of the droplets in the interaction between the spray and the ambient gas.

4. Conclusions

An analysis on the evaporating diesel spray structure was conducted and the particle image velocimetry (PIV) was used in this study. The following conclusions are drawn from this study.

Ambient-gas flow can be observed using a PIV in high temperature · high pressure field, and the size of the macro vortex flow that exist in the downstream region of the evaporative diesel free spray is found to be 30 % of the length spray penetration, irrespective of the injection pressure.

In the case of the same mass of the injected fuel in the inner spray, the spray tip penetration does not depend on the change of injection pressure.

In the case of evaporative diesel free spray, the increase of injection pressure causes the ambient gas flow to become more irregular. As a result, mixture formation is promoted by the increase of injection pressure.

Acknowledgments

This study was supported by research funds from Dong-A University.

Nomenclature

L : Spray Tip Penetration
 P : Pressure
 T : Temperature
 V : Droplets Velocity
 Z : Distance from Nozzle Tip

Greek symbols

Φ : Diameter
 ρ : Density
 ω : Vorticity

Subscripts

a : Ambient
 inj : Injection
 liq : Liquid phase
 R : Radial direction

References

- [1] H. Ando, Key word for power train development of the future car, *Journal of Society of Automotive Engineers of Japan*, 54 (7) (2000) 7-9.
- [2] M. Shioji, T. Kimoto, M. Okamoto and M. Ikegami, 1998, An analysis of diesel flame by picture processing, *Transactions of the Japan Society of Mechanical Engineers series B*, 54 (504) (1998) 2228-2235.
- [3] N. Fujitani, New diesel fuel injection, Diesel fuel injection workshop, Sankaido, (1997) 191-198.
- [4] T. Dan, Turbulent structure and formation mechanism of diesel sprays, Doshisha University Doctoral Thesis, Japan, (1996).
- [5] J. K. Yeom, T. Takahashi, T. Tanaka, S. Kusano, J. Senda and H. Fujiomoto, The structure analysis of impinging and free diesel spray with exciplex fluorescence method in high temperature and pressure field, The 15th Internal Combustion Engine Symposium (International) In Seoul, (22) (1997) 117-122.
- [6] T. Soeda, M. Ota and S. Omatsu, Fundamental and application of mathematical statistics, Nissin Publication, Japan, (1992) 177-178.
- [7] M. Takarazawa, M. Toada, K. Kikuchi, T. Yonemoto and T. Tsukada, Diffusion and transport phenomena, Baifukan, (1996) 123-125.
- [8] S. Takagishi, T. Takahashi, T. Dan, J. Senda and H.

- Fujimoto, Analysis of flow field in diesel fuel sprays by particle-image velocimetry, *Transactions of the Japan Society of Mechanical Engineers series B*, 65(631) (1999) 1128-1133.
- [9] T. Tanaka, Analysis on inner structure and mixture formation process in unsteady evaporating diesel sprays, Doshisha University Master's Thesis, Japan, (2000).
- [10] T. Takahashi, Analysis on the vaporization, dispersion and mixing process in unsteady diesel spray, Doshisha University Master's Thesis, Japan, (1999).